Back to the Basics: Two Approaches for the Identification and Extraction of Lipid Droplets from *Malassezia pachydermatis* CBS1879 and *Malassezia globosa* CBS7966

Maria Juliana Mantilla,[1,6] Catherine Eliana Cabrera Díaz,[2,6] Gabriela Ariza-Aranguren,[1] Hans de Cock,[3] J. Bernd Helms,[4] Silvia Restrepo,[5] Elizabeth Jiménez,[2] and Adriana Marcela Celis Ramírez[1,7]

[1]Grupo de Investigación Celular y Molecular de Microorganismos Patógenos (CeMoP), Department of Biological Sciences, Universidad de Los Andes, Bogotá, Colombia
[2]Applied Biochemistry Research Group (GIBA), Department of Chemistry, Universidad de Los Andes, Bogotá, Colombia
[3]Microbiology, Department of Biology, Faculty of Science, Institute of Biomembranes, Utrecht University, Utrecht, The Netherlands
[4]Department of Biomolecular Health Sciences, Utrecht University, Utrecht, The Netherlands
[5]Laboratorio de Micología y Fitopatología (LAMFU), Chemical and Food Engineering Department, Universidad de Los Andes, Bogotá, Colombia
[6]These authors contributed equally to this work.
[7]Corresponding author: *acelis@uniandes.edu.co*

Malassezia spp. are lipid-dependent yeasts that have been related to skin mycobiota and dermatological and systemic diseases. Study of lipid droplets (LDs) is relevant to elucidate the unknown role of these organelles in *Malassezia* and to gain a broader overview of lipid metabolism in *Malassezia*. Here, we standardized two protocols for the analysis of LDs in *M. pachydermatis* and *M. globosa*. The first describes co-staining for confocal laser-scanning fluorescence microscopy, and the second details extraction and purification of LDs. The double stain is achieved with three different neutral lipid fluorophores, namely Nile Red, BODIPY™ 493/503, and HCS LipidTOX™ Deep Red Neutral, in combination with Calcofluor White. For LD extraction, cell wall rupture is conducted using *Trichoderma harzianum* enzymes and cycles of vortexing with zirconium beads. LD purification is performed in a three-step ultracentrifugation process. These standardizations will contribute to the study of the dynamics, morphology, and composition of LDs in *Malassezia.* © 2021 Wiley Periodicals LLC.

Basic Protocol 1: Lipid droplet fluorescence staining
Basic Protocol 2: Lipid droplet extraction and purification
Support Protocol: *Malassezia* spp. culture conditions

Keywords: cell wall rupture • fluorescence microscopy • lipid droplets • *Malassezia globosa* • *Malassezia pachydermatis*

How to cite this article:
Mantilla, M. J., Cabrera Díaz, C. E., Ariza-Aranguren, G., Helms, J. B., Restrepo, S., Jiménez, E., & Celis Ramírez, A. M. (2021). Back to the basics: Two approaches for the identification and extraction of lipid droplets from *Malassezia pachydermatis* CBS1879 and *Malassezia globosa* CBS7966. *Current Protocols*, *1,* e122. doi: 10.1002/cpz1.122

CURRENT PROTOCOLS
A Wiley Brand
Current Protocols e122, Volume 1
Published in Wiley Online Library (wileyonlinelibrary.com).
doi: 10.1002/cpz1.122

INTRODUCTION

Malassezia spp. are lipophilic and lipid-dependent yeasts associated with skin mycobiota of human and animals (Cabañes, 2014; Chang et al., 1998; Czyzewska et al., 2016). This genus includes 18 species (Lorch et al., 2018) associated with skin disorders (Cabañes, 2014; Grice & Dawson Jr., 2017; Hay & Midgley, 2010), fungemia in neonates and immunocompromised patients (Cabañes, 2014; Guého-Kellermann, Boekhout, & Begerow, 2010; Hay & Midgley, 2010), and more recently Crohn's disease, exacerbation of colitis, Parkinson disease, and pancreatic ductal adenocarcinoma (Aykut et al., 2019; Laurence, Benito-León, & Calon, 2019; Limon et al., 2019).

Knowledge of lipid metabolism in these yeast species is scarce, and many processes of its pathophysiology are yet to be understood (Mayser & Gaitanis, 2010). *Malassezia* spp. cannot synthesize lipids (fatty acids, or FAs) due to a lack of genes encoding the cytosolic fatty acid synthase complex (FAS). Thus, the sebum, a lipid-rich substance produced by the sebaceous glands of humans and animals, is an essential source of nutrients (Grice & Dawson Jr., 2017; Ro & Dawson, 2005) for these yeasts. *Malassezia* spp. possess a high number of genes encoding secreted enzymes such as lipases and phospholipases, which can degrade the sebum. In turn, these enzymes can also cause damage to the host (Mayser & Gaitanis, 2010). Degraded lipids outside the cell enter the yeast cell and participate in different intracellular metabolic processes, such as elongation, β-oxidation, or storage (Celis Ramírez et al., 2020; Klug & Daum, 2014; Mayser & Gaitanis, 2010).

Lipid storage is carried out by lipid droplets (LDs). These organelles contain a core of neutral lipids, such as triglycerides and sterol esters, which is surrounded by a phospholipid monolayer and proteins (Walther & Farese, 2012). LDs have been reported in most biological models from bacteria to mammals, including humans cells (Zhang & Liu, 2017). LDs have been shown to fulfill biological functions such as participating in membrane organization and dynamics, energy homeostasis, energy storage, lipid metabolism, and signal transduction (Olzmann & Carvalho, 2019) and helping cells to buffer fluctuations in energy availability (Sui et al., 2018). Organisms control the number and size of these organelles depending on internal or external signals such as the concentration of lipids (Yang, Galea, Sytnyk, & Crossley, 2012).

Studies on these organelles have been conducted in different fields (Onal, Kutlu, Gozuacik, & Dokmeci Emre, 2017; Walther & Farese, 2012). In medicine, LDs have attracted special interest due to their association with several pathologies, and in biotechnology, LDs in yeasts such as *Pichia pastoris* and *Saccharomyces cerevisiae* and some grains like oatmeal are used for biofuel production (Aguilar et al., 2017; Walther & Farese, 2012).

LDs have become a subject of study in *Malassezia* to gain information about lipid metabolism in this genus. Lipidomic analysis of these organelles in *M. furfur* revealed the presence of phospholipids and triglycerides (Celis et al., 2018). Lipid storage is possibly involved in the pathogenic behavior of this yeast (Henne, Reese, & Goodman, 2018; Onal et al., 2017; Radulovic et al., 2013). LDs are promoters of pathogenicity such as that occurring in *Mycobacterium tuberculosis* (Armstrong, Carter, Atkinson, Terhune, & Zahrt, 2018) or are promotors of survival under different types of stress, as observed in *Rhodococcus jostii* (Zhang & Liu, 2017). They are also involved in the assembly of viral particles during hepatic steatosis development in hepatitis C (Ferguson et al., 2017; Herker & Ott, 2012; Miyanari et al., 2007).

Here, we standardized two protocols for the analysis of *M. pachydermatis* CBS1879 and *M. globosa* CBS7966 LDs to evaluate their structure and composition. Basic Protocol 1 describes co-staining with different fluorophores for confocal laser-scanning microscopy,

allowing the identification of LD morphology. Basic Protocol 2 describes the extraction and purification of LDs, allowing analysis of the composition. In addition, we describe the methodology that is used to culture the two strains (Support Protocol).

CAUTION: M. pachydermatis CBS1879 and *M. globosa* CBS7966 are Biosafety Level 2 (BSL-2) pathogens. Follow all appropriate guidelines and regulations for the use and handling of pathogenic microorganisms.

LIPID DROPLET FLUORESCENCE STAINING

BASIC PROTOCOL 1

Confocal laser-scanning microscopy is a valuable tool to assess LD morphology (Ding et al., 2013). Here, we present a standardized methodology for LD morphology identification in *Malassezia* spp. based on a double-stain fluorescence microscopy with Calcofluor White combined with three different neutral lipid fluorophores: Nile Red, BODIPY^{TM} 493/503, and HCS LipidTOX^{TM} Deep Red Neutral; to our knowledge, this is the first double-staining protocol for LDs in this genus. Fluorescence staining methods used in other yeasts, such as *S. cerevisiae* and *Rhodotorula minuta*, for LD observation use comparable concentrations of fluorophores and fixation agents as the ones used here (Adeyo et al., 2011; Patel, Pruthi, & Pruthi, 2019; Wolinski & Kohlwein, 2008; Zhu et al., 2015). However, to adapt the staining procedure to this genus, the following changes were introduced in this protocol: (i) neutral lipid fluorophore incubation times are higher than the ones used in other yeasts (Adeyo et al., 2011; Patel et al., 2019; Wolinski & Kohlwein, 2008; Zhu et al., 2015), and (ii) the incubation temperature was adjusted to 30°C, which prevents changes observed in environmental temperature, allowing method reproducibility.

Materials

M. pachydermatis CBS1879 or *M. globosa* CBS7966 grown to early stationary phase (see Support Protocol)
Sterile phosphate-buffered saline (PBS), pH 7.4
4% (w/v) paraformaldehyde (in water)
1 mg ml^{-1} Nile Red (e.g., Sigma-Aldrich, cat. no. 72485) in methanol
0.1 mg ml^{-1} BODIPY^{TM} 493/503 (e.g., Invitrogen, cat. no. D3922) in methanol
100× HCS LipidTOX^{TM} Deep Red Neutral (e.g., Invitrogen, cat. no. H34477) in dimethyl sulfoxide (DMSO)
0.01% (v/v) Calcofluor White (e.g., Sigma-Aldrich, cat. no. 18909; in water)
10% (w/v) KOH (in water)

1.5-ml microcentrifuge tubes
Microcentrifuge
Aluminum foil
Vortex
30°C shaking incubator
Glass microscope slides
Coverslips
Clear nail polish
Confocal laser-scanning microscope (e.g., Olympus FV1000) with 60×/1.42 NA oil-immersion objective
Microscope software (e.g., Olympus FluoView, version 4.1)
ImageJ, version 2.0.0-rc-69/1.52p (*www.fiji.sc*)

Cell neutral lipid staining

1. Collect three aliquots of 1 ml *M. pachydermatis* CBS1879 or *M. globosa* CBS7966 grown to early stationary phase (see Support Protocol) in individual 1.5-ml microcentrifuge tubes.

2. Wash each aliquot three times with 1 ml sterile PBS, pH 7.4. For each washing step, centrifuge tubes for 5 min at 5000 × *g*. After the last wash step, centrifuge tubes for 5 min at 5000 × *g* and reserve pellet.

3. Resuspend pellet at room temperature in 100 µl of 4% paraformaldehyde to fix the cells. Immediately add 2 µl of each of the following fluorochromes to different tubes: 1 mg ml^{-1} Nile Red in methanol, 0.1 mg ml^{-1} BODIPY™ 493/503 in methanol, or 100× HCS LipidTOX™ Deep Red Neutral in DMSO. Cover tubes with aluminum foil and vortex for 15 s.

   Each fluorochrome is added to a single microcentrifuge tube.

   From this point, make sure to keep the 1.5-ml microcentrifuge tubes in darkness.

4. Incubate cells in the dark for 2 hr in a 30°C shaking incubator at 52 rpm.

5. Wash cells by adding 1 ml sterile PBS, pH 7.4, and centrifuging 3 min at 1248 × *g*.

6. Thoroughly resuspend cells in 100 µl of 4% paraformaldehyde.

   Cells can be stored ≤1 day at 4°C after the staining procedure and before visualization.

Cell wall staining and microscopy visualization

7. Place 2 µl of the previously neutral lipid–stained cells on a clean glass microscope slide.

   Make at least three slides per stained tube. To avoid cell agglomeration on the slides, vortex the cells before staining.

8. Place 2 µl of 0.01% Calcofluor White and 2 µl of 10% KOH on top of cells on the slides and let slides dry for 1 to 2 min.

   Letting the slides dry before putting the coverslip on (step 9) helps to avoid cell movement during visualization.

9. Put a coverslip on top of sample and seal borders with clear nail polish.

   Clear nail polish prevents movement of the coverslip during confocal imaging (steps 10 to 12).

   Slides can be stored ≤2 days at 4°C before visualization.

10. Visualize cells with a confocal laser-scanning microscope using the following settings:

    a. For Calcofluor White, the DAPI settings.
    b. For Nile Red, the Alexa 488 settings.
    c. For BODIPY™ 493/503, use the FITC settings.
    d. For HCS LipidTOX™ Deep Red Neutral, the Alexa 633 settings.

    Calcofluor White is used to stain the fungal cell wall, and Nile Red, BODIPY™ 493/503, and HCS LipidTOX™ Deep Red Neutral are utilized for LD visualization.

11. Use a 60×/1.42 NA oil-immersion objective and a digital zoom of 4× to take images under Calcofluor White and neutral lipid fluorophore settings.

12. Obtain Z-stacks at 1024 × 1024 pixels (55 × 55 µm), imaging every 0.5 µm.

    The number of stack images should be between 15 and 30 images. Make sure the stack images cover the whole cell. We recommend obtaining at minimum three Z-stacks at different locations on each slide.

13. Analyze raw data, obtained as .oib files, using the microscope software.

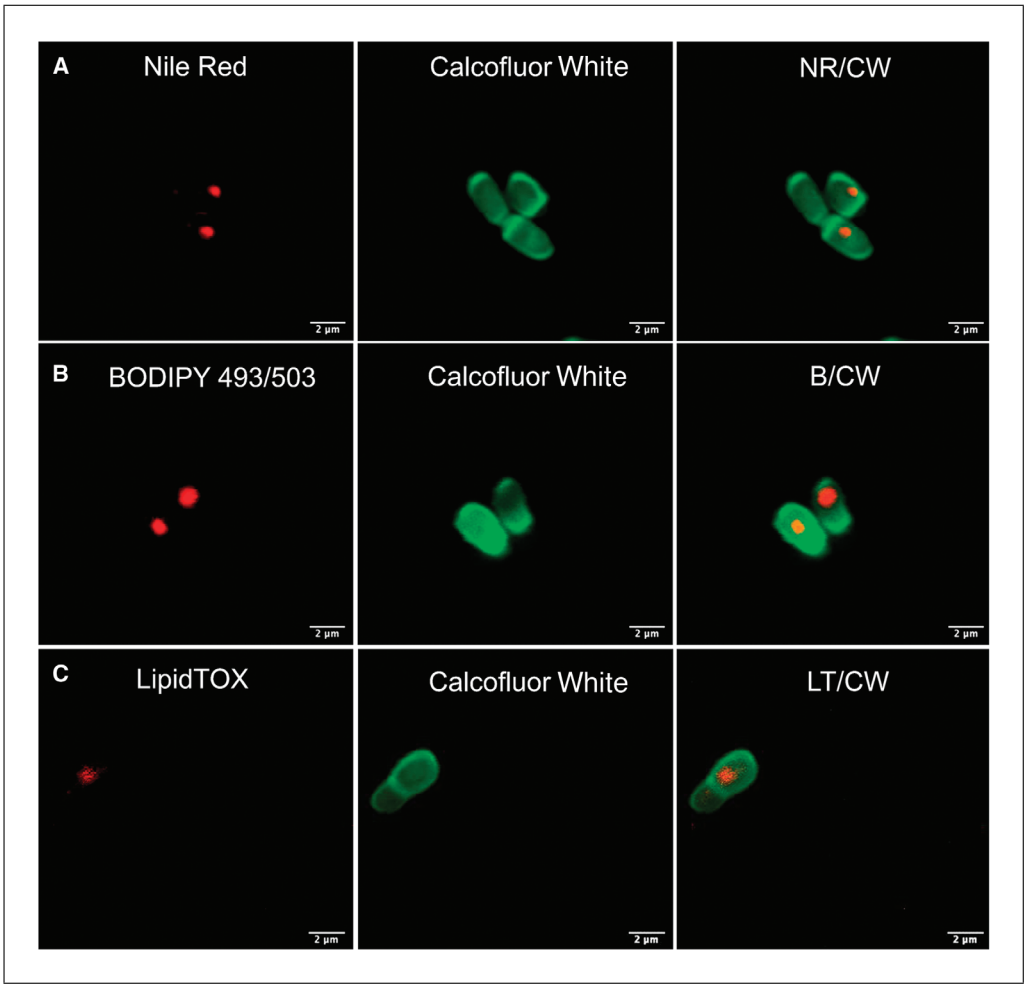

Figure 1 Co-staining of LDs and *M. pachydermatis* CBS1879 (after 30 hr of incubation, early stationary phase) with the following fluorophores: (**A**) Nile Red (red) and Calcofluor White (green), (**B**) BODIPY™ 493/503 (red) and Calcofluor White (green), and (**C**) HCS LipidTOX™ Deep Red Neutral (red) and Calcofluor White (green). Scale bar 2 µm. Representative maximum-intensity projections are shown for *M. pachydermatis* cells and LDs.

14. Using ImageJ, overlay Calcofluor White and neutral lipid fluorophore .oib files to generate top views of each of the stacks and observe the contrast between the cell wall and the LDs.

    This can be achieved using the project stacks function in ImageJ software (Fig. 1 and 2). In the figures, for each image, Z-stacks were used to create maximum-intensity projections with the function "Z project" in ImageJ. All neutral lipid staining images were combined with each corresponding cell wall staining image with the function "merge channel." To add a scale bar, use the following workflow: Analyze > Tools > Scale bar.

    For suggestions to resolve common problems with this protocol, see Table 1.

LIPID DROPLET EXTRACTION AND PURIFICATION

BASIC PROTOCOL 2

Removal of the cell wall and subsequent lysis of the spheroplast without damaging LDs is one of the most critical steps to obtain these organelles (Radulovic et al., 2013). Several methodologies, such as enzymatic, chemical, and mechanical procedures, have been used to perform the rupture in other biological models, but in most cases, cell breakage is accomplished with only one of the aforementioned protocols (see Current Protocols article; Brasaemle & Wolins, 2016; Ding et al., 2013; Mannik, Meyers, & Dalhaimer, 2014). For example, for *Ustilago maydis*, an enzymatic reaction of 45 min was sufficient

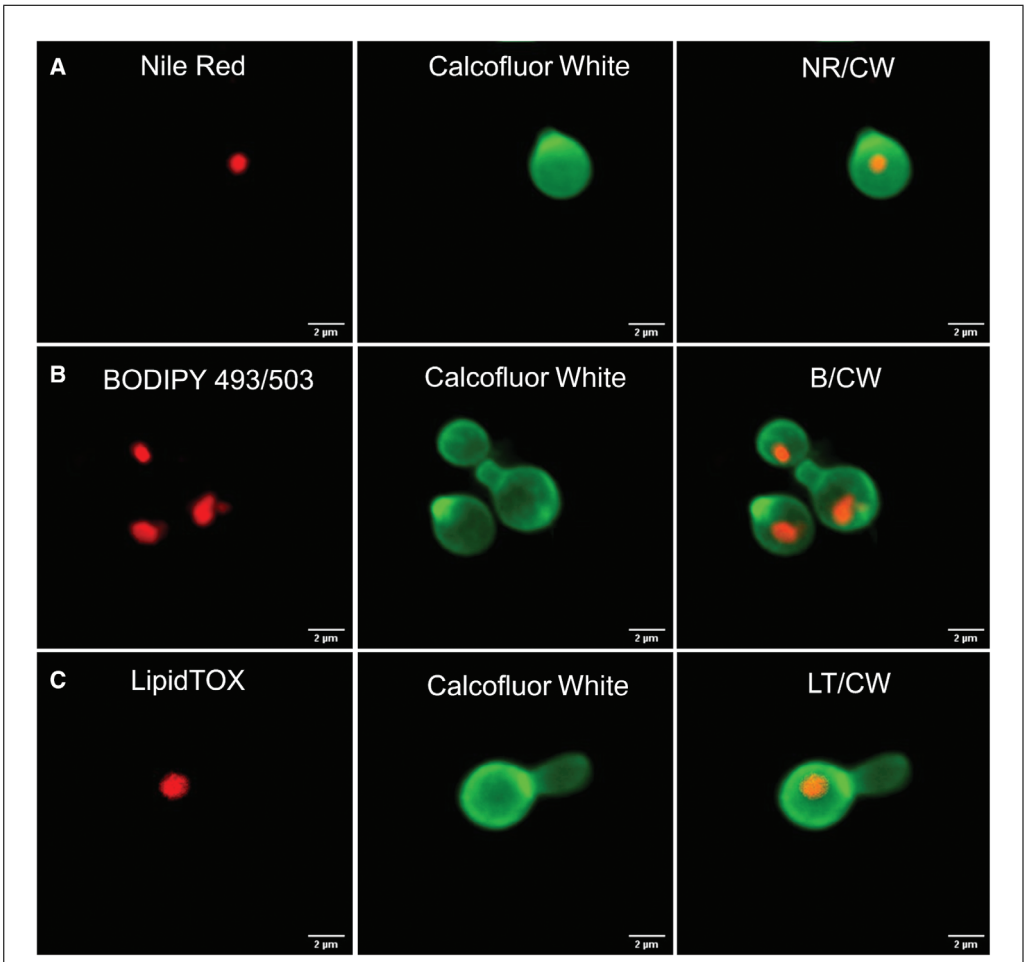

Figure 2 Co-staining of LDs and *M. globosa* CBS7966 (after 72 hr of incubation, early stationary phase) with the following fluorophores: (**A**) Nile Red (red) and Calcofluor White (green), (**B**) BODIPY™ 493/503 (red) and Calcofluor White (green), and (**C**) HCS LipidTOX™ Deep Red Neutral (red) and Calcofluor White (green). Scale bar 2 µm. Representative maximum-intensity projections are shown for *M. globosa* cells and LDs.

Table 1 Suggestions for Overcoming Possible Problems with Lipid Droplet Fluorescence Staining

Possible problem	Suggestion for overcoming problem
Agglomeration of cells on the slide	Increase the duration of vortexing of the cells before adding them to the slide.
Cells moving on the slide	Increase the drying time of the slide before sealing the coverslip.
Neutral lipid fluorophores photobleaching in confocal imaging	Decrease the laser intensity. Increase the stack distance to increase the imaging speed. Avoid exposure of the slides to light.

to generate cell wall rupture (Aguilar et al., 2017). To achieve cell wall rupture in our work, we combine the use of four different techniques, which include (i) enzymatic reaction for 18 hr, a longer time than used in other protocols (Aguilar et al., 2017; Mannik et al., 2014), and cycles of mechanical rupture by (ii) addition of zirconium beads, (iii) vortexing, and (iv) Dounce homogenization. To further improve the rupture, we perform the homogenization during the growth phase of the yeast cells, taking into consideration the structure of the *Malassezia* cell wall (Guého-Kellermann et al., 2010; Mittag, 1995), which is reported to thicken in later stationary phases (Pomraning et al., 2015).

Additional Materials *(also see Basic Protocol 1)*

Lytic enzymes from *Trichoderma harzianum* (e.g., Sigma-Aldrich, cat. no. L1412)
600 mM $(NH_4)_2SO_4$ (e.g., Sigma-Aldrich, cat. no. A4915)
Wash buffer (see recipe)
Buffers A, B, and C (see recipe)
0.5-mm zirconium beads
mDixon agar plates (see recipe)

50-ml centrifuge tubes
47°C shaking incubator
Standard tabletop centrifuge
Dounce homogenizer with loose-fitting glass pestle
24-ml polycarbonate ultracentrifuge bottles (Thermo Fisher Scientific)
Sorvall™ WX ultracentrifuge (Thermo Fisher Scientific) with Fiberlite™ F37L-8 × 39 Fixed-Angle Rotor (Thermo Fisher Scientific), 4°C
33°C incubator

Conversion to spheroplasts

1. Begin enzymatic digestion of cell wall in a 50-ml centrifuge tube by combining a preparation of lytic enzymes from *T. harzianum* at a concentration of 16 mg g^{-1} wet weight in 600 mM $(NH_4)_2SO_4$ (Mannik et al., 2014) with *M. pachydermatis* CBS1879 or *M. globosa* CBS7966 grown to early stationary phase (see Support Protocol).

   For the digestion, use ∼4.16 mg enzymes in 5 ml buffer for each 13 ml medium (mDixon medium) containing yeast (M. pachydermatis or M. globosa).

2. Incubate digestion in a 47°C shaking incubator at 52 rpm for 18 hr.

3. After the incubation, wash cells twice with 10 ml wash buffer and recover by centrifuging 5 min at 3000 × *g*.

4. Resuspend at a ratio of 1 ml g^{-1} wet weight in Buffer A.

   The resuspension is in ∼10 ml Buffer A.

5. Add 0.92 g of 0.5-mm zirconium beads for mechanical disruption and perform cycles of vortexing for 1 min and then incubating for 30 s on ice.

   For M. pachydermatis, 30 cycles are necessary, and for M. globosa, 50 cycles.

6. Stroke sample 120 times with a Dounce homogenizer with a loose-fitting glass pestle (Ding et al., 2013; Mannik et al., 2014).

7. Dilute homogenate with 0.5 volumes of Buffer A and centrifuge 10 min at 6000 × *g*. Store supernatant at 4°C in a new 50-ml centrifuge tube.

8. Resuspend pellet in 0.5 volumes of Buffer A with 120 strokes with the Dounce homogenizer and centrifuge 10 min at 6000 × *g* (Ding et al., 2013; Mannik et al., 2014).

   Add the same volume of Buffer A as was used in step 7. Keep an aliquot of ≥2 ml at 4°C for further evaluation of the process (step 18).

Lipid droplet extraction

9. Combine supernatants from steps 7 and 8 in one or two 24-ml polycarbonate ultracentrifuge bottles (depending on the supernatant volume) to one-third of the capacity and add Buffer A to 80% of the capacity.

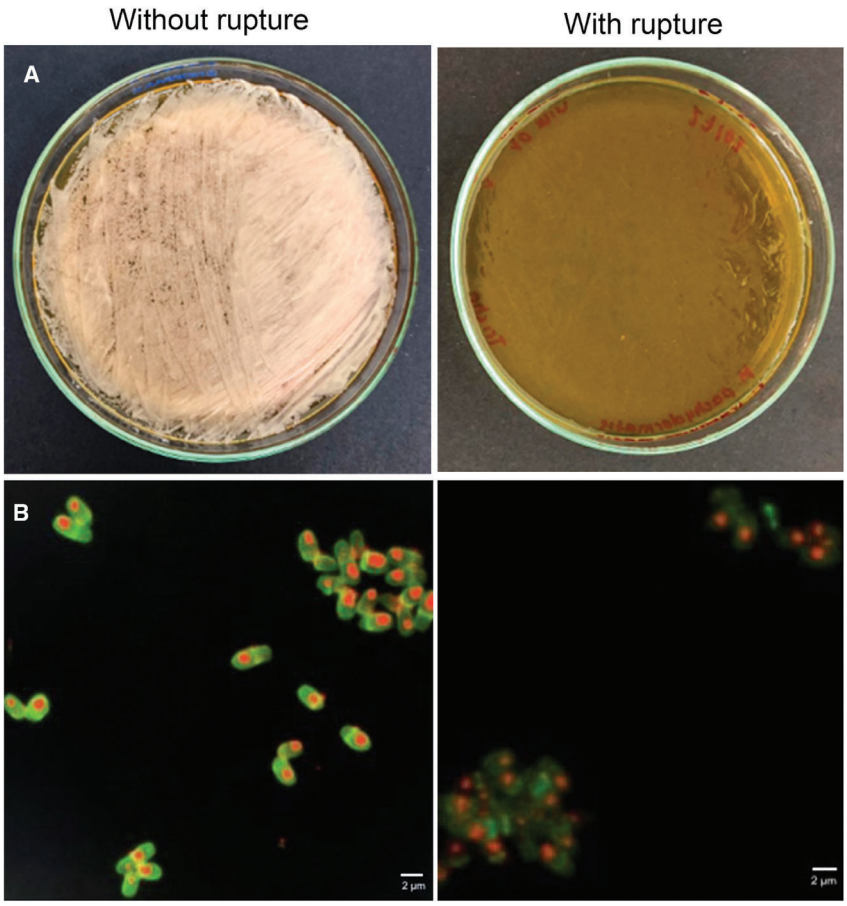

Figure 3 Evaluation of rupture in the *M. pachydermatis* cell wall by (**A**) culture on mDixon agar and (**B**) co-staining with Nile Red (red) and Calcofluor White (green), scale bar 2 µm. Left panels, control sample (without rupture). Right panels, after enzymatic digestion and chemical disruption. Representative maximum-intensity projections are shown for *M. pachydermatis* lysis.

Here and in steps 12 and 15, balance the bottles (two bottles of supernatant or one bottle plus a balance) to within 0.01 g.

10. Ultracentrifuge 1 hr at 182,000 × *g*, 4°C, in a Sorvall™ WX ultracentrifuge with a Fiberlite™ F37L-8 × 39 Fixed-Angle Rotor.

11. Recover resulting top layer with a micropipet and transfer it to a new polycarbonate bottle.

    Avoid moving the bottle because the top layer can be dispersed. Expect ~4 ml sample. Keep a 0.5- to 1-ml aliquot at 4°C for further evaluation of the process (step 18).

12. Fill tube to 80% of the capacity with Buffer B and homogenize with 10 strokes with Dounce homogenizer.

13. Ultracentrifuge 1 hr at 182,000 × *g*, 4°C.

14. Recover resulting top layer with a micropipet and transfer it to a new polycarbonate bottle.

    Avoid moving the bottle because the top layer can be dispersed. Expect ~4 ml sample. Keep a 0.5- to 1-ml aliquot at 4°C for further evaluation of the process (step 18).

15. Add Buffer C to three-quarters of the capacity and homogenize with 10 strokes with Dounce homogenizer.

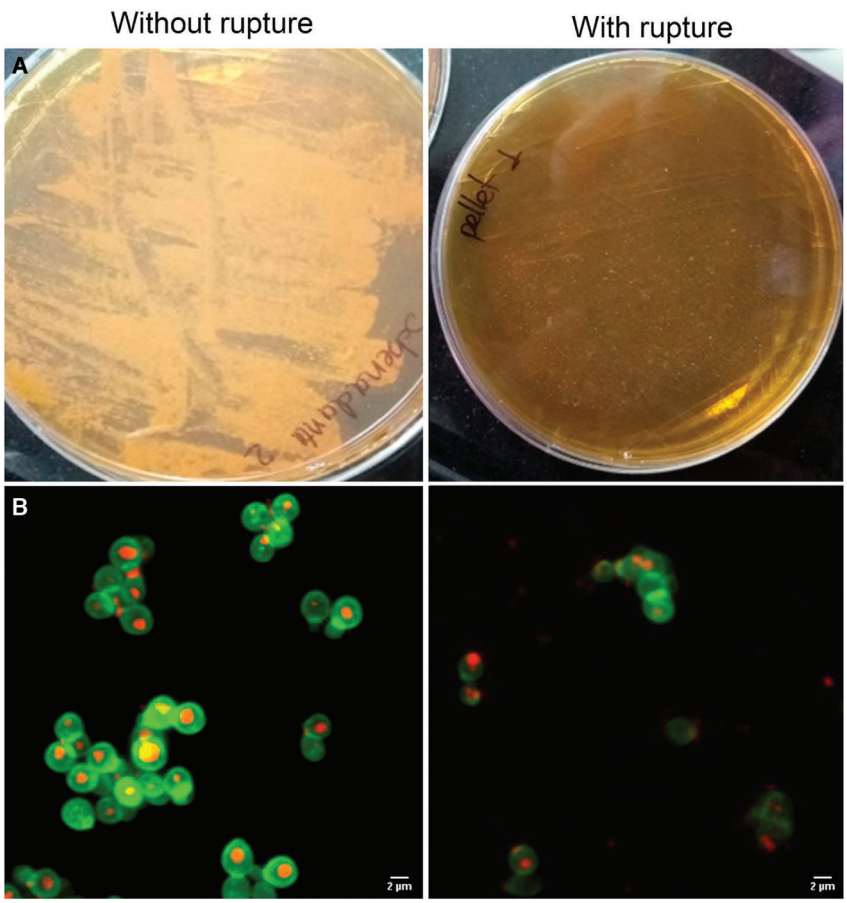

Figure 4 Evaluation of rupture in the *M. globosa* cell wall by (**A**) culture on mDixon agar and (**B**) co-staining with Nile Red (red) and Calcofluor White (green), scale bar 2 μm. Left panels, control sample (without rupture). Right panels, after enzymatic digestion and chemical disruption. Representative maximum-intensity projections are shown for *M. globosa* lysis.

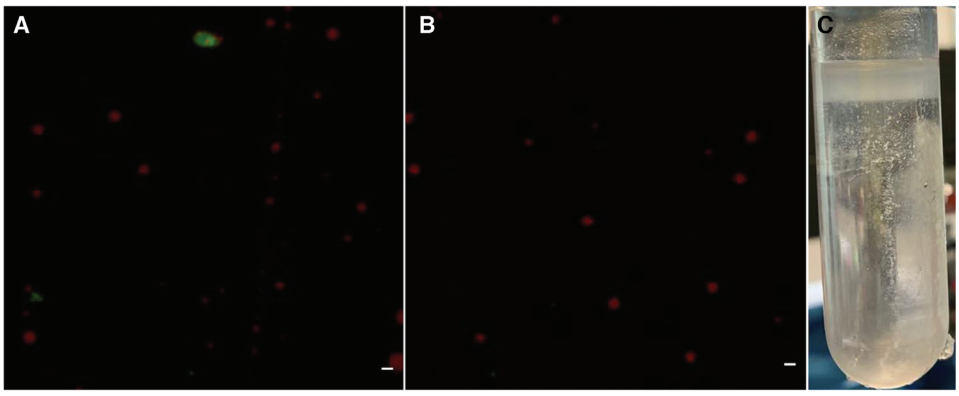

Figure 5 Evaluation of the LD purification process by co-staining with Nile Red (red) and Calcofluor White (green). (**A**) Supernatant from the first ultracentrifugation step and (**B**) top layer from the third ultracentrifugation step. Scale bar 2 μm. Representative maximum-intensity projections are shown for LD purification. (**C**) Ultracentrifuge tube after the last step of the purification process.

Table 2 Suggestions for Overcoming Possible Problems with Lipid Droplet Extraction and Purification

Possible problem	Suggestion for overcoming problem
Ficoll® 400 insolubility	Dilute small quantities with the help of a vortex and sonicator bath.
Spheroplasts are not obtained	Increase the number of cycles of vortexing with beads and placing on ice or the number of strokes with the Dounce homogenizer.
No LDs are obtained after ultracentrifugation or the supernatant does not resemble a milky solution	Review the steps for breaking the cell wall (mechanical and enzymatic) to check that the droplets have not broken; if this happens, the enzyme reaction time or cycles must be reduced. If the problem is not in the formation of spheroplasts, change the time or speed of the ultracentrifugation. For more information, see Ding et al. (2013).

16. Ultracentrifuge 1 hr at 182,000 × *g*, 4°C.
17. Collect top layer (containing the LDs), transfer to a new 50-ml centrifuge tube, and store at 4°C.

    Avoid moving the bottle because the top layer can be dispersed. Expect ∼4 ml sample. The top layer should be a milky solution at the top of ultracentrifugation bottle; this is the purified LD fraction. Keep a 0.5- to 1-ml aliquot at 4°C for further evaluation of the process (step 18).

18. For evaluation of the process, use aliquots stored in steps 8, 11, 14, and 17. For the aliquot from step 8, culture 1 ml on an mDixon agar plate at 33°C for 7 days. For all aliquots, stain 1 ml with Nile Red and Calcofluor White to visualize with fluorescence microscopy (see Basic Protocol 1 and see Fig. 3 and 4 for the pre-ultracentrifugation sample and Fig. 5 for the post-ultracentrifugation samples).

    If the LDs are not going to be used right after the extraction, it is recommended to lyophilize them and store them at room temperature.

    For suggestions to resolve common problems with this protocol, see Table 2.

SUPPORT PROTOCOL

Malassezia spp. CULTURE CONDITIONS

Malassezia is a genus of lipophilic and lipid-dependent yeasts found in the microbiota of humans and warm-blooded animals (Lorch et al., 2018). These yeasts colonize the sebaceous glands to obtain its nutrients from the sebum, a lipid-rich substance (Cabañes, 2014). Their lipid-dependence phenotype makes these species difficult to cultivate. Therefore, special lipid-abundant media such as modified Dixon are used in order to achieve *Malassezia* culture.

Materials

M. pachydermatis CBS1879 or *M. globosa* CBS7966 (Westerdijk Fungal Biodiversity Institute, The Netherlands, *https://wi.knaw.nl*)
mDixon agar plates (see recipe)
0.1% (v/v) Tween 80 (in water)
mDixon medium (see recipe)

33°C incubator
Sterile inoculating loops
Sterile 125-ml flasks
33°C shaking incubator

1. Two to three weeks in advance of assays (see Basic Protocols 1 and 2), streak *M. pachydermatis* CBS1879 or *M. globosa* CBS7966 from stock onto mDixon agar

plates. Incubate plates at 33°C for 72 to 96 hr for *M. pachydermatis* and 1 week for *M. globosa*.

This time could change depending on the strain.

2. Streak 1 to 2 colonies on new mDixon agar plates using sterile inoculating loops and incubate them at 33°C for 48 to 72 hr for *M. pachydermatis* and 96 to 108 hr for *M. globosa*.
3. Suspend colonies from these plates in 3 ml of 0.1% Tween 80 and adjust inoculum to standard of 2 on the McFarland scale.
4. Add suspension to 27 ml mDixon medium in a sterile 125-ml flask. Grow in a 33°C shaking incubator at 180 rpm for 72 hr for *M. pachydermatis* and 108 hr for *M. globosa*.
5. Inoculate 0.3 ml of the growth strain into 29.7 ml fresh mDixon medium in a sterile 125-ml flask and grow for 30 hr for *M. pachydermatis* and 72 hr for *M. globosa*.

In this experiment, Malassezia strains are grown up to early stationary phase. Growth times may be varied to achieve other growth phases.

REAGENTS AND SOLUTIONS

Buffer A

10 mM MES/Tris (e.g., Sigma-Aldrich, cat. no. M2933 and 252859), pH 6.9
12% (w/v) Ficoll® 400 (e.g., Sigma-Aldrich, cat. no. F8016)
0.2 mM EDTA (e.g., Sigma-Aldrich, cat. no. E6758E6758)
1 mM phenylmethylsulfonyl fluoride (PMSF; e.g., AMRESCO, cat. no. M145)
Store ≤1 day at 4°C

This buffer can be prepared in advance if the PMSF is not added; incorporate this reactive the day that the buffer is going to be used.

Prepare a stock of 0.2 M PMSF by dissolving 0.35 g PMSF in 10 ml DMSO and then divide the solution into 1-ml aliquots and store them at −20°C in the dark. When adding the PMSF to the buffer, adjust the volume according to the final concentration needed and the total volume of buffer prepared.

Buffer B

8% (w/v) Ficoll® 400 (e.g., Sigma-Aldrich, cat. no. F8016)
10 mM MES/Tris (e.g., Sigma-Aldrich, cat. no. M2933 and 252859), pH 6.9
0.2 mM $Na_2EDTA{\cdot}2H_2O$ (e.g., Sigma-Aldrich, cat. no. E4884)
Store ≤1 week at 4°C

Buffer C

0.25 M sorbitol (e.g., Sigma-Aldrich, cat. no. S1876)
10 mM MES/Tris (e.g., Sigma-Aldrich, cat. no. M2933 and 252859), pH 6.9
0.2 mM $Na_2EDTA{\cdot}2H_2O$ (e.g., Sigma-Aldrich, cat. no. E4884)
Store ≤1 week at 4°C

Modified Dixon (mDixon) agar plates

36 g L^{-1} Mycosel agar (e.g., BD, cat. no. B11462)
20 g L^{-1} ox bile (e.g., Sigma-Aldrich, cat. no. 70168)
36 g L^{-1} malt extract (e.g., Oxoid, cat. no. LP0039)
2 ml L^{-1} glycerol (e.g., Sigma-Aldrich, cat. no. G5516)
2 ml L^{-1} oleic acid (e.g., Sigma-Aldrich, cat. no. O1383)
10 ml L^{-1} Tween 40 (e.g., Sigma-Aldrich, cat. no. P1504)
Pour plates and store ≤2 weeks at 4°C

Make sure that the agar plates are at room temperature before use.

Modified Dixon (mDixon) medium

36 g L^{-1} malt extract (e.g., Oxoid, cat. no. LP0039)
6 g L^{-1} peptone (e.g., BD, cat. no. 211677)
20 g L^{-1} ox bile (e.g., Sigma-Aldrich, cat. no. 70168)
2 ml L^{-1} glycerol (e.g., Sigma-Aldrich, cat. no. G5516)
2 ml L^{-1} oleic acid (e.g., Sigma-Aldrich, cat. no. O1383)
10 ml L^{-1} Tween 40 (e.g., Sigma-Aldrich, cat. no. P1504)
Store ≤2 weeks at 4°C

Make sure that the medium is at room temperature before use.

Wash buffer

400 mM sucrose (e.g., Sigma-Aldrich, cat. no. 84097)
10 mM Tris (e.g., Sigma-Aldrich, cat. no. 252859)
1 mM EDTA (e.g., Sigma-Aldrich, cat. no. E6758)
Adjust to pH 7.0 with NaOH
Store ≤1 week at 4°C

COMMENTARY

Background Information

Culturing

We have presented common growth conditions for *M. pachydermatis* and *M. globosa* strains (Support Protocol). mDixon medium is a lipid-abundant medium that can be stored after preparation for ∼2 weeks at 4°C.

Confocal imaging

Different techniques are available to study the morphology and composition of LDs in other biological models. Some of the main approaches in the study of LDs are fluorescence microscopy and lipidomic analysis. As lipids do not possess intrinsic fluorescence, fluorophores with affinity for different types of lipids have been used, allowing the observation and determination of LD morphology and dynamics (Daemen, van Zandvoort, Parekh, & Hesselink, 2016).

For neutral lipids present in LDs, Nile Red, BODIPY™ 493/503, and HCS LipidTOX™ Deep Red Neutral have been used (Daemen et al., 2016; Eggert, Rösch, Reimer, & Herker, 2014; Govender, Ramanna, Rawat, & Bux, 2012; Olzmann & Carvalho, 2019; Walther & Farese, 2012). These fluorophores have different advantages and disadvantages that were determined in different organisms for which the stains have been assessed for the study of LDs, such as in microalgae, yeasts, and mammalian cells (Daemen et al., 2016; Feng et al., 2013; Olzmann & Carvalho, 2019; Wang et al., 2010).

Dual stains allow one both to observe individual LDs and to identify individual cells. In Basic Protocol 1, double staining includes cell wall staining with Calcofluor White, a well-known fluorophore used for this purpose because it binds to chitin, a component of the cell wall (Guého-Kellermann et al., 2010; Harrington & Hageage, 2003; Ram & Klis, 2006; Stalhberger et al., 2014). This is a blue-emitting fluorophore (λ_{em} < 500 nm) having an excitation around 365 nm and an emission spectra peak around 440 nm, which prevents spectra overlapping with those of the other fluorophores used in this work (Fam, Klymchenko, & Collot, 2018; Knox, 2012).

Lipid droplet extraction assays

A second approach to study LDs is lipidomic analysis, which determines the lipid composition of these organelles (Ivashov et al., 2013), but this approach requires the extraction and purification of LDs to implement the analysis (Ding et al., 2013; Radulovic et al., 2013). Even though various methods have been reported for the study of LDs, to the extent of our knowledge, these have not been described for *Malassezia.* Considering the morphological characteristics, specifically the thickness and multilamellar structure of the cell wall, and the metabolic characteristics of these yeast species, it is of great importance to have protocols available for the study of these organelles.

Different methods have been used to confirm the efficiency of cell rupture and

extraction and purification of LDs. The most common analysis methods consist of staining with fluorophores to determine some qualitative characteristics and observation of the position, color, and consistency of the top layer in the ultracentrifuge bottle (Aguilar et al., 2017; see Current Protocols article; Brasaemle & Wolins, 2016; Ding et al., 2013; Mannik et al., 2014). In Basic Protocol 2, we use two methods for verification of cell rupture: culture on mDixon agar and Nile Red staining. These techniques confirm the degradation of the cell wall and lysis of the spheroplasts, one of the most critical steps in standardization. After cell breakage, it was expected that the staining procedure would show LDs with a round morphology, at the outside of the cell or in close proximity to it (Aguilar et al., 2017; Brasaemle & Wolins, 2016; Ding et al., 2013; Mannik et al., 2014). As for the final product after LD purification, it was expected that LDs would be recovered at the top of the ultracentrifuge tube due to their low density and with a color and consistency resembling a milky solution (Brasaemle & Wolins, 2016; Ding et al., 2013; Gao et al., 2017; Mannik et al., 2014). The results that we obtained were consistent with previously mentioned reports on LD purification. One of the most frequent problems that can occur during purification protocols is loss of these organelles (Brasaemle & Wolins, 2016; Ding et al., 2013; Gao et al., 2017). Because of this and to determine whether LDs were still available at the end of the process, all the ultracentrifugation steps were qualitatively monitored. It was possible to establish that the standardized protocol allowed the recovery of LDs to carry out a compositional analysis using lipidomic approaches (such as ultra-performance liquid chromatography–mass spectrometry, or UPLC-MS; M. J. Mantilla et al., unpub. observ.).

Critical Parameters and Troubleshooting

Culturing

Standard microbiology sterile techniques are critical for all protocols in this article. In all protocols, one or more uninoculated negative controls should be used to verify that the medium has not been contaminated.

Confocal imaging and lipid droplet extraction assays

See Tables 1 and 2 for troubleshooting suggestions.

Understanding Results

Confocal imaging

Standardization of a dual-staining protocol for LDs and the cell wall of *M. pachydermatis* and *M. globosa* for confocal imaging (Basic Protocol 1) was achieved. The procedure, with three different neutral lipid fluorophores (Nile Red, BODIPY, and LipidTOX, observed in red), was optimized. Calcofluor White (observed in green) was used to stain the cell wall of the yeast (Fig. 1 and 2). The three different neutral lipid fluorophores efficiently stained *M. pachydermatis* and *M. globosa* LDs, even though there were some small differences. The image resolution for LDs from *M. pachydermatis* (Fig. 1) as well as the staining stability was better when the imaging was carried out with Nile Red, as compared to LipidTOX and BODIPY. For *M. globosa*, the same staining pattern was observed (Fig. 2). The Nile Red staining procedure reported here was successful and allowed the observation of LDs, regardless of some challenges reported in the literature (Fam et al., 2018). BODIPY LD imaging also showed good organelle definition, demonstrating a good selectivity and resolution (Collot et al., 2018; Fam et al., 2018; Yang, Hsu, Yang, & Yang, 2012). In contrast, LipidTOX showed lower resolution compared with Nile Red and BODIPY staining. This is possibly due to staining problems in smaller LDs (Camus, Vogt, Kondratowicz, & Ott, 2013) or the lack of stability of this fluorophore (Ranall, Gabrielli, & Gonda, 2011; Stalhberger et al., 2014).

Conversion to spheroplasts and lipid droplet extraction

The protocol to achieve cell rupture of *M. pachydermatis* and *M. globosa* in order to extract and purify LDs (Basic Protocol 2) was optimized. The rupture efficiency was evaluated by two different methods: culture on mDixon agar (Fig. 3A and 4A), which established that the cell wall was affected enough to prevent the yeast from further growth, and fluorescence co-staining (Fig. 3B and 4B), which showed affected cell walls because the signal emission was less bright. In some cases, the morphology of the cell was poorly defined. Additionally, some LDs were present outside the cell or near the edge of the cell.

The purification process was evaluated after each ultracentrifugation step by fluorescence co-staining of LDs and cell walls. As is shown in Figure 5A and 5B, a reduction in the quantity of the *Malassezia* cell wall was

observed during the subsequent steps of purification. At the same time, LDs remained present during the entire purification process. Additionally, throughout the purification process for 30 ml of yeast culture, a white layer with a volume of ∼4 ml was observed at the top of the ultracentrifuge tube during each density centrifugation step (Fig. 5C), indicating the presence of LDs (Ding et al., 2013; Mannik et al., 2014).

Time Considerations

M. pachydermatis and *M. globosa* culturing (Support Protocol) might take 2 to 3 weeks before the actual assays (Basic Protocols 1 and 2). The dual-staining protocol for both strains (Basic Protocol 1) takes 4 to 6 hr without taking into account the imaging visualization and the culture of *M. pachydermatis* or *M. globosa*. Conversion of *M. pachydermatis* or *M. globosa* to spheroplasts takes 22 to 24 hr, including the incubation time with the lytic enzymes of *T. harzianum* (Basic Protocol 2). LD extraction (Basic Protocol 2) takes 7 to 9 hr without taking into account the 7 days of incubation on mDixon agar and the microscopy observation, which can take 2 to 3 hr depending on the number of slides. In addition, making the buffers and reagents requires 3 to 5 hr.

Acknowledgments

This work was supported by the Faculty of Sciences, Universidad de Los Andes, grant no. INV-2018-31-1252, Project Semilla INV-2018-49-1371, Project FAPA-P17160322012, and the Vice-Presidency of Research and Creation. We thank μ-core at Universidad de Los Andes (*https://microcore.uniandes.edu.co/es/*).

Author Contributions

Maria Juliana Mantilla: Data curation, Formal analysis, Investigation, Methodology, Validation, Visualization, Writing-original draft, Writing-review & editing, Catherine Eliana Cabrera Díaz: Data curation, Formal analysis, Investigation, Methodology, Validation, Visualization, Writing-original draft, Writing-review & editing, Gabriela Ariza-Aranguren: Investigation, Methodology, Writing-review & editing, Hans de Cock: Conceptualization, Methodology, Writing-review & editing, J. Bernd Helms: Conceptualization, Methodology, Writing-review & editing, Silvia Restrepo: Funding acquisition, Resources, Writing-review & editing, Elizabeth Jiménez: Funding acquisition, Resources, Writing-review & editing, Adriana Marcela Celis Ramírez: Conceptualization, Formal analysis, Funding acquisition, Methodology, Project administration, Resources, Supervision, Validation, Writing-review & editing

Conflict of Interest

The authors declare that the research was conducted in the absence of any commercial or financial relationships that could be construed as a potential conflict of interest.

Data Availability Statement

Data sharing not applicable–no new data generated.

Literature Cited

Adeyo, O., Horn, P. J., Lee, S., Binns, D. D., Chandrahas, A., Chapman, K. D., & Goodman, J. M. (2011). The yeast lipin orthologue Pah1p is important for biogenesis of lipid droplets. *The Journal of Cell Biology*, *192*, 1043–1055. doi: 10.1083/jcb.201010111.

Aguilar, L. R., Pardo, J. P., Lomelí, M., Bocardo, O. I. L., Oropeza Juárez, M., & Sánchez Guerra, G. (2017). Lipid droplets accumulation and other biochemical changes induced in the fungal pathogen *Ustilago maydis* under nitrogen–starvation. *Archives of Microbiology*, *199*, 1195–1209. doi: 10.1007/s00203-017-1388-8.

Armstrong, R. M., Carter, D. C., Atkinson, S. N., Terhune, S. S., & Zahrt, T. C. (2018). Association of *Mycobacterium* proteins with lipid droplets. *Journal of Bacteriology*, *200*, e00240–e00218. doi: 10.1128/JB.00240-18.

Aykut, B., Pushalkar, S., Chen, R., Li, Q., Abengozar, R., Kim, J. I., … Miller, G. (2019). The fungal mycobiome promotes pancreatic oncogenesis via activation of MBL. *Nature*, *574*, 264–267. doi: 10.1038/s41586-019-1608-2.

Brasaemle, D., & Wolins, N. (2016). Isolation of lipid droplets from cells by density gradient centrifugation. *Current Protocols in Cell Biology*, *72*, 3.15.1–3.15.13.

Cabañes, F. J. (2014). *Malassezia* yeasts : How many species infect humans and animals? *PLOS Pathogens*, *10*, e1003892. doi: 10.1371/journal.ppat.1003892.

Camus, G., Vogt, D. A., Kondratowicz, A. S., & Ott, M. (2013). Lipid droplets and viral infections. In H. Yang & P. Li (Eds.), *Methods in cell biology* (pp. 167–190). Academic Press. doi: 10.1016/B978-0-12-408051-5.00009-7.

Celis Ramírez, A. M., Amezquita, A., Cardona, J., Matiz-Cerón, L. F., Andrade-Martinez, J. S., Triana, S., … de Cock, H. (2020). Analysis of *Malassezia* lipidome disclosed differences among the species and reveals presence of unusual yeast lipids. *Frontiers in Cellular and Infection Microbiology*, *10*, 338. doi: 10.3389/fcimb.2020.00338.

Celis, A. M., Triana, S., Ibarra, H., Cardona, J., Restrepo, S., Gonzalez, A., … de Cock, H.

(2018, June/July). *Identification and characterization of lipid droplets in Malassezia furfur*. Paper presented at the Congress of the International Society for Human and Animal Mycology, Amsterdam, Netherlands. Abstract retrieved from https://www.morressier.com/article/identification-characterization-lipid-droplets-malassezia–furfur/5ac39997d462b8028d89a22a

Chang, H., Miller, H., Watkins, N., Arduino, M., Ashford, D., Midgle, G., … Jarvis, W. R. (1998). An epidemic of *Malassezia pachydermatis* in an intensive care nursery associated with colonization of health care workers' pet dogs. *New England Journal of Medicine*, *338*, 706–711. doi: 10.1056/NEJM199803123381102.

Collot, M., Fam, T. K., Ashokkumar, P., Faklaris, O., Galli, T., Danglot, L., & Klymchenko, A. S. (2018). Ultrabright and fluorogenic probes for multicolor imaging and tracking of lipid droplets in cells and tissues. *Journal of the American Chemical Society*, *140*, 5401–5411. doi: 10.1021/jacs.7b12817.

Czyzewska, U., Siemieniuk, M., Pyrkowska, A., Nowakiewicz, A., Bieganska, M., Dabrowska, I., … Tylicki, A. (2016). Comparison of lipid profiles of *Malassezia pachydermatis* strains isolated from dogs with otitis externa and without clinical symptoms of disease. *Mycoses*, *59*, 20–27. doi: 10.1111/myc.12429.

Daemen, S., van Zandvoort, M. A. M. J., Parekh, S. H., & Hesselink, M. K. C. (2016). Microscopy tools for the investigation of intracellular lipid storage and dynamics. *Molecular Metabolism*, *5*, 153–163. doi: 10.1016/j.molmet.2015.12.005.

Ding, Y., Zhang, S., Yang, L., Na, H., Zhang, P., Zhang, H., … Liu, P. (2013). Isolating lipid droplets from multiple species. *Nature Protocols*, *8*, 43–51. doi: 10.1038/nprot.2012.142.

Eggert, D., Rösch, K., Reimer, R., & Herker, E. (2014). Visualization and analysis of hepatitis C virus structural proteins at lipid droplets by super-resolution microscopy. *PLOS One*, *9*, e102511. doi: 10.1371/journal.pone.0102511.

Fam, T., Klymchenko, A., & Collot, M. (2018). Recent advances in fluorescent probes for lipid droplets. *Materials*, *11*, 1768. doi: 10.3390/ma11091768.

Feng, G. D., Zhang, F., Cheng, L. H., Xu, X. H., Zhang, L., & Chen, H. L. (2013). Evaluation of FT-IR and Nile Red methods for microalgal lipid characterization and biomass composition determination. *Bioresource Technology*, *128*, 107–112. doi: 10.1016/j.biortech.2012.09.123.

Ferguson, D., Zhang, J., Davis, M. A., Helsley, R. N., Vedin, L. L., Lee, R. G., … Brown, J. M. (2017). The lipid droplet-associated protein perilipin 3 facilitates hepatitis C virus-driven hepatic steatosis. *Journal of Lipid Research*, *58*, 420–432. doi: 10.1194/jlr.M073734.

Gao, Q., Binns, D. D., Kinch, L. N., Grishin, N. V., Ortiz, N., Chen, X., & Goodman, J. M. (2017). Pet10p is a yeast perilipin that stabilizes lipid droplets and promotes their assembly. *The Journal of Cell Biology*, *216*, 3199–3217. doi: 10.1083/jcb.201610013.

Govender, T., Ramanna, L., Rawat, I., & Bux, F. (2012). BODIPY staining, an alternative to the Nile Red fluorescence method for the evaluation of intracellular lipids in microalgae. *Bioresource Technology*, *114*, 507–511. doi: 10.1016/j.biortech.2012.03.024.

Grice, E. A., & Dawson, Jr. T. L. (2017). Host – microbe interactions : *Malassezia* and human skin. *Current Opinion in Microbiology*, *40*, 81–87. doi: 10.1016/j.mib.2017.10.024.

Guého-Kellermann, E., Boekhout, T., & Begerow, D. (2010). Biodiversity, phylogeny and ultrastructure. In A. Velegraki (Ed.), *Malassezia and the skin: Science and clinical practice* (pp. 17–63). Berlin: Springer. doi: 10.1007/978-3-642-03616-3_2.

Harrington, B. J., & Hageage, G. J. (2003). Calcofluor white: A review of its uses and applications in clinical mycology and parasitology. *Laboratory Medicine*, *34*, 361–367. doi: 10.1309/EPH2TDT8335GH0R3.

Hay, R., & Midgley, G. (2010). Introduction: *Malassezia* yeasts from a historical perspective. In A. Velegraki (Ed.), *Malassezia and the skin: Science and clinical practice* (pp. 1–16). Berlin: Springer. doi: 10.1007/978-3-642-03616-3_1.

Henne, W. M., Reese, M. L., & Goodman, J. M. (2018). The assembly of lipid droplets and their roles in challenged cells. *EMBO Journal*, *37*, e98947. doi: 10.15252/embj.201898947.

Herker, E., & Ott, M. (2012). Emerging role of lipid droplets in host /pathogen interactions. *The Journal of Biological Chemistry*, *287*, 2280–2287. doi: 10.1074/jbc.R111.300202.

Ivashov, V. A., Grillitsch, K., Koefeler, H., Leitner, E., Baeumlisberger, D., Karas, M., & Daum, G. (2013). Lipidome and proteome of lipid droplets from the methylotrophic yeast *Pichia pastoris*. *BBA - Molecular and Cell Biology of Lipids*, *1831*, 282–290. doi: 10.1016/j.bbalip.2012.09.017.

Klug, L., & Daum, G. (2014). Yeast lipid metabolism at a glance. *FEMS Yeast Research*, *14*, 369–388. doi: 10.1111/1567-1364.12141.

Knox, J. P. (2012). In situ detection of cellulose with carbohydrate-binding modules. In H. J. Gilbert (Ed.), *Methods in enzymology* (pp. 233–245). Academic Press. doi: B978-0-12-415931-0.00012-4.

Laurence, M., Benito-León, J., & Calon, F. (2019). *Malassezia* and Parkinson's disease. *Frontiers in Neurology*, *10*, 758. doi: 10.3389/fneur.2019.00758.

Limon, J. J., Tang, J., Li, D., Wolf, A. J., Michelsen, K. S., Funari, V., … Underhill, D. M. (2019). *Malassezia* is associated with Crohn's disease and exacerbates colitis in mouse models. *Cell Host and Microbe*, *25*, 377–388. doi: 10.1016/j.chom.2019.01.007.

Lorch, J. M., Palmer, J. M., Vanderwolf, K. J., Schmidt, K. Z., Verant, M. L., Weller,

T. J., & Blehert, D. S. (2018). *Malassezia vespertilionis* sp. nov.: A new cold-tolerant species of yeast isolated from bats. *PERSOONIA - Molecular Phylogeny and Evolution of Fungi*, *41*, 56–70. doi: 10.3767/persoonia.2018.41.04.

Mannik, J., Meyers, A., & Dalhaimer, P. (2014). Isolation of cellular lipid droplets: Two purification techniques starting from yeast cells and human placentas. *Journal of Visualized Experiments*, *86*, 1–10. doi: 10.3791/50981.

Mayser, P., & Gaitanis, G. (2010). Physiology and biochemistry. In A. Velegraki (Ed.), *Malassezia and the skin: Science and clinical practice* (pp. 121–137). Berlin: Springer. doi: 10.1007/978-3-642-03616-3_4.

Mittag, H. (1995). Fine structural investigation of *Malassezia furfur.* II. The envelope of the yeast cells. *Mycoses*, *38*, 13–21. doi: 10.1111/j.1439-0507.1995.tb00003.x.

Miyanari, Y., Atsuzawa, K., Usuda, N., Watashi, K., Hishiki, T., Zayas, M., … Shimotohno, K. (2007). The lipid droplet is an important organelle for hepatitis C virus production. *Nature Cell Biology*, *9*, 1089–1097. doi: 10.1038/ncb1631.

Olzmann, J., & Carvalho, P. (2019). Dynamics and functions of lipid droplets. *Nature Reviews Molecular Cell Biology*, *20*, 137–155. doi: 10.1038/s41580-018-0085-z.

Onal, G., Kutlu, O., Gozuacik, D., & Dokmeci Emre, S. (2017). Lipid droplets in health and disease. *Lipids in Health and Disease*, *16*, 128. doi: 10.1186/s12944-017-0521-7.

Patel, A., Pruthi, V., & Pruthi, P. A. (2019). Innovative screening approach for the identification of triacylglycerol accumulating oleaginous strains. *Renewable Energy*, *135*, 936–944. doi: 10.1016/j.renene.2018.12.078.

Pomraning, K. R., Wei, S., Karagiosis, S. A., Kim, Y. M., Dohnalkova, A. C., Arey, B. W., … Baker, S. E. (2015). Comprehensive metabolomic, lipidomic and microscopic profiling of *Yarrowia lipolytica* during lipid accumulation identifies targets for increased lipogenesis. *PLOS One*, *10*, 0123188. doi: 10.1371/journal.pone.0123188.

Radulovic, M., Knittelfelder, O., Cristobal-Sarramian, A., Kolb, D., Wolinski, H., & Kohlwein, S. D. (2013). The emergence of lipid droplets in yeast: Current status and experimental approaches. *Current Genetics*, *59*, 231–242. doi: 10.1007/s00294-013-0407-9.

Ram, A. F. J., & Klis, F. M. (2006). Identification of fungal cell wall mutants using susceptibility assays based on Calcofluor white and Congo red. *Nature Protocols*, *1*, 2253–2256. doi: 10.1038/nprot.2006.397.

Ranall, M., Gabrielli, B., & Gonda, T. (2011). High-content imaging of neutral lipid droplets with 1,6-diphenylhexatriene. *BioTechniques*, *50*, 35–42. doi: 10.2144/000113702.

Ro, B. I., & Dawson, T. L. (2005). The role of sebaceous gland activity and scalp microfloral metabolism in the etiology of seborrheic dermatitis and dandruff. *The Journal of Investigative Dermatology. Symposium Proceedings*, *10*, 194–197. doi: 10.1111/j.1087-0024.2005.10104.x.

Stalhberger, T., Simenel, C., Clavaud, C., Eijsink, V. G. H., Jourdain, R., Delepierre, M., … Fontaine, T. (2014). Chemical organization of the cell wall polysaccharide core of *Malassezia restricta*. *Journal of Biological Chemistry*, *289*, 12647–12656. doi: 10.1074/jbc.M113.547034.

Sui, X., Arlt, H., Brock, K. P., Lai, Z. W., Dimaio, F., Marks, D. S., … Walther, T. C. (2018). Cryo-electron microscopy structure of the lipid droplet-formation protein seipin. *Journal of Cell Biology*, *217*, 4080–4091. doi: 10.1083/jcb.201809067.

Walther, T. C., & Farese, R. V. (2012). Lipid droplets and cellular lipid metabolism. *Annual Review of Biochemistry*, *81*, 687–714. doi: 10.1146/annurev-biochem-061009-102430.

Wang, H., Wei, E., Quiroga, A., Sun, X., Touret, N., & Lehner, R. (2010). Altered lipid droplet dynamics in hepatocytes lacking triacylglycerol hydrolase expression. *Molecular Biology of the Cell*, *21*, 1991–2000. doi: 10.1091/mbc.e09-05-0364.

Wolinski, H., & Kohlwein, S. D. (2008). Microscopic analysis of lipid droplet metabolism and dynamics in yeast. In A. Vancura (Ed.), *Methods in molecular biology* (pp. 151–163). Totowa, NJ: Human Press. doi: 10.1007/978-1-59745-261-8_11.

Yang, H., Galea, A., Sytnyk, V., & Crossley, M. (2012). Controlling the size of lipid droplets : Lipid and protein factors. *Current Opinion in Cell Biology*, *24*, 509–516. doi: 10.1016/j.ceb.2012.05.012.

Yang, H.-J., Hsu, C.-L., Yang, J.-Y., & Yang, W.-Y. (2012). Monodansylpentane as a blue-fluorescent lipid-droplet marker for multi-color live-cell imaging. *PLOS One*, *7*, e32693. doi: 10.1371/journal.pone.0032693.

Zhang, C., & Liu, P. (2017). The lipid droplet: A conserved cellular organelle. *Protein and Cell*, *8*, 796–800. doi: 10.1007/s13238-017-0467-6.

Zhu, Z., Ding, Y., Gong, Z., Yang, L., Zhang, S., Zhang, C., … Zhao, Z. K. (2015). Dynamics of the lipid droplet proteome of the oleaginous yeast *Rhodosporidium toruloides*. *Eukaryotic Cell*, *14*, 252–264. doi: 10.1128/EC.00141-14.